

Double symmetry breaking of solitons in one-dimensional virtual photonic crystals

Yongyao Li^{1,4,*}, Boris A. Malomed^{2,3}, Mingneng Feng¹, and Jianying Zhou^{1†}

¹*State Key Laboratory of Optoelectronic Materials and Technologies,
Sun Yat-sen University, Guangzhou 510275, China*

²*Department of Physical Electronics, School of Electrical Engineering,
Faculty of Engineering, Tel Aviv University, Tel Aviv 69978, Israel*

³*ICFO-Institut de Ciències Fòniques, Mediterranean Technology Park, 08860 Castelldefels (Barcelona), Spain*

⁴*Department of Applied Physics, South China Agricultural University, Guangzhou 510642, China*

We demonstrate that spatial solitons undergo two consecutive spontaneous symmetry breakings (SSBs), with the increase of the total power, in nonlinear photonic crystals (PhCs) built as arrays of alternating linear and nonlinear stripes, in the case when maxima of the effective refractive index coincide with minima of the self-focusing coefficient, and vice versa, i.e., the corresponding linear and nonlinear periodic potentials are in competition. This setting may be induced, as a *virtual* PhC, by means of the EIT (electromagnetically-induced-transparency) technique, in a uniform optical medium. It may also be realized as a Bose-Einstein condensate (BEC) subject to the action of combined periodic optical potential and periodically modulated Feshbach resonance. The first SSB happens at the center of a linear stripe, pushing a broad low-power soliton into an adjacent nonlinear stripe and gradually suppressing side peaks in the soliton's shape. Then, the soliton restores its symmetry, being pinned to the midpoint of the nonlinear stripe. The second SSB occurs at higher powers, pushing the narrow soliton off the center of the nonlinear channel, while the soliton keeps its internal symmetry. The results are obtained by means of numerical and analytical methods. They may be employed to control switching of light beams by means of the varying power.

PACS numbers: 42.65.Tg; 42.70.Qs; 05.45.Yv; 03.75.Lm

I. INTRODUCTION

It is commonly known that linear eigenstates supported by symmetric potentials, in contexts such as quantum mechanics and photonic crystals (PhCs), may be classified according to representations of the underlying symmetry group [1]. The addition of the nonlinearity frequently gives rise to the effect of the spontaneous symmetry breaking (SSB), i.e., reduction of the full symmetry group to its subgroups, in the generic situation. The basic feature of the SSB is the transition from the symmetric ground state (GS) to that which does not follow the symmetry of the potential. The simplest manifestations of the SSB, which were predicted in early works [2], and then in the model of nonlinear dual-core optical fibers [3, 4], occur in settings based on symmetric double-well potentials, or similarly designed nonlinear *pseudopotentials* [5] (the latter name for effective potentials induced by a spatially inhomogeneous nonlinearity is used in solid-state physics [6]). In the quantum theory, the nonlinearity naturally appears in the context of the mean-field description of Bose-Einstein condensates (BECs), with the Schrödinger equation replaced by the Gross-Pitaevskii equation [7]. Similarly, the self-focusing makes PhCs a medium in which the linear symmetry competes with the nonlinearity, in two-dimensional (2D) [8] and 1D [9]-[12] settings.

A natural extension of the SSB in the double-well potential is the transition from symmetric to asymmetric solitons in the geometry which adds a uniform transverse dimension to the potential, extending the potential from the double well into a double trough. In this setting, the soliton self-traps in the free direction due to the self-focusing nonlinearity. The SSB effect in the solitons may be described by means of the effectively 1D two-mode approximation, which is tantamount to the usual temporal-domain model of dual-core optical fibers [4], and may also be applied to the BEC loaded into a pair of parallel tunnel-coupled cigar-shaped traps [13]. In the application to the BEC, a more accurate description of the symmetry-broken solitons was developed too, in the framework of the 2D Gross-Pitaevskii equation, for the linear [14] and nonlinear [15] double-trough potentials.

PhC media are modeled by combinations of linear and nonlinear potentials, which correspond to the alternation of material elements and voids in the PhC structure [8]-[12]. A similar setting, emulating the PhC, may be induced by means of the electromagnetically-induced-transparency (EIT) technique in a uniform medium [16]. For BEC, a counterpart of the PhC may be generated as a combination of the linear potential, induced by the optical lattice,

*Electronic address: yongyaoli@gmail.com

†Electronic address: stszjy@mail.sysu.edu.cn

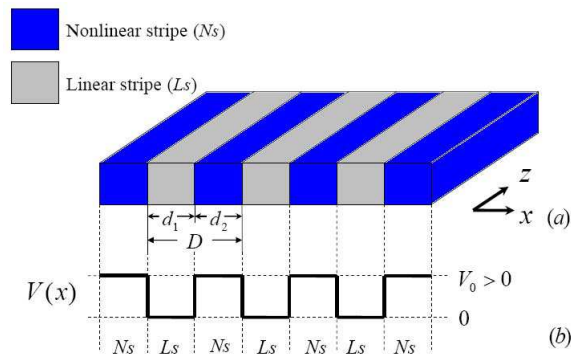


FIG. 1: (Color online) (a) The scheme of the virtual photonic crystal with period $D = d_1 + d_2$. The blue (darker) and gray (lighter) slabs represent the nonlinear and linear stripes, respectively. (b) The corresponding Kronig-Penney modulation function.

and a nonlinear pseudopotential imposed by a periodically patterned magnetic or optical field modifying the local nonlinearity via the Feshbach-resonance effect. Actually, the latter setting may be more general than the PhC, as the so designed linear and nonlinear potentials may be created with incommensurate periodicities [17].

Solitons in periodic linear and nonlinear potentials have been studied theoretically in many works, as reviewed in Refs. [18] and [19]. In particular, specific types of *gap solitons* were predicted in 1D models of PhCs featuring the competition between the periodically modulated refractive index and *self-defocusing* material nonlinearity [12]. Spatial optical solitons, supported by effective linear potentials, were created in various experimental setups [20].

Unlike the double-well settings, periodic potentials usually do not give rise to SSB in solitons, although examples of asymmetric solitons were found in some 1D models [11]. Indeed, 1D optical media built as periodic alternations of self-focusing material elements and voids feature no competition between the effective linear and nonlinear potentials, as minima and maxima of both types of the potentials coincide, hence there is no drive for the SSB in the medium (as mentioned above, the competition takes place if the material nonlinearity is self-defocusing, but in that case the corresponding gap solitons do not feature SSB either [12]). Competing potentials leading to SSB effects might be possible if maxima of the refractive index would correspond to minima of the self-focusing nonlinearity. While this is impossible in usual PhCs, composed of material stripes separated by voids, the effective potential structures induced by EIT patterns in uniform media admit such a situation [16] (as said above, a similar setting is also possible in BEC [17, 19]). The objective of this work is to study the SSB for spatial solitons in the *virtual* PhC of this type, following the gradual increase of the total power of the soliton. It will be demonstrated that the symmetry breaking happens twice in this setting, first to a low-power soliton centered around a midpoint of a linear channel, and then to a high-power beam situated at the center of the nonlinear stripe.

The setting under the consideration is displayed in Fig. 1(a), obeying the following version of the nonlinear Schrödinger equation for local amplitude $V(x, z)$, which is a function of propagation distance z and transverse coordinate x :

$$iu_z = -(1/2)u_{xx} + V(x)(1 - |u|^2)u, \quad (1)$$

where the Kronig-Penney (KP) potential function, $V(x)$, is defined as per Fig. 1(b). We stress that the self-focusing sign of the nonlinearity makes the model different from ones with the competition between the linear and nonlinear potentials provided by the self-defocusing [12]. We consider the version of the system with $d_1 = d_2 \equiv d$ in Fig. 1(a).

The scaling is fixed by setting the modulation depth to be $V_0 = 0.02$, which leaves half-period d of the potential as a free parameter. In Section 2, we present numerical results, at first, for $d = 10$, which illustrates a generic situation. Then, we demonstrate the results for other values of the period, namely, $d = 5, 8, 11$, and 14 . In particular, it will be demonstrated that the second SSB vanishes at large values of d . In Section 3, we report analytical approximations,

II. SOLITONS AND THEIR SYMMETRY BREAKINGS (NUMERICAL RESULTS)

A. Results for $d = 10$

GS (ground-state) solutions to Eq. (1) with the above-mentioned values of the parameters, $d_1 = d_2 = 10$ and $V_0 = 0.02$, were found by means of the imaginary-time-propagation method [21]. Characteristic features of GS solitons,

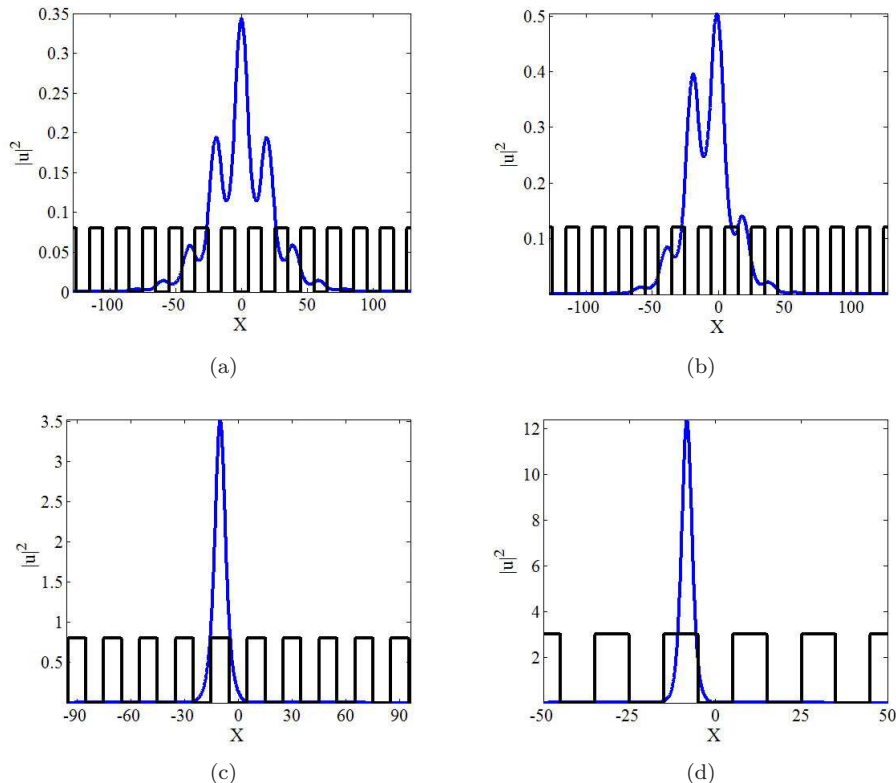


FIG. 2: (Color online) Profiles of ground-state solitons found at the following values of the total power: $P = 12$ (a), $P = 16$ (b), $P = 29$ (c), and $P = 50$ (d).

which distinguish them from bound complexes of two or several solitary beams, is the presence of a pronounced central peak, and the absence of nodes (zero crossings).

Figure 2 displays a characteristic set of GS profiles found at different values of total power, which is defined as $P = \int_{-\infty}^{+\infty} |u(x)|^2 dx$. Representing the stationary solutions as $u(x, z) = e^{-i\mu z} U(x)$, it is straightforward to check that wavenumber $-\mu$ of all the GS solitons falls into the semi-infinite gap, in terms of the spectrum generated by the linearized version of Eq. (1), see Fig. 3(d) below; this situation is natural for the system with the self-focusing nonlinearity. Further, real-time simulations of Eq. (1) (not shown here) demonstrates that all the GS modes are stable against perturbations. As seen from Fig. 3(d), the stability of the GS solitons is also supported by the *Vakhitov-Kolokolov criterion* [23], $d\mu/dP < 0$.

At sufficiently small values of P (in the weakly nonlinear regime), Fig. 2(a) demonstrates that the central and side peaks of the GS soliton are situated in linear channels, the soliton being symmetric about its central peak, which exactly coincides with the midpoint of the corresponding linear stripe. Although the light is chiefly guided by the linear stripes in this regime, the soliton of course cannot exist without the self-focusing nonlinearity, even if it is weak.

As seen in Fig. 2(b), the first SSB event happens with the increase of P , breaking the symmetry of the weakly-nonlinear GS soliton and spontaneously shifting its central peak off the center of the linear channel in which the peak is trapped. The symmetry of the side peaks gets broken too, although they remain trapped in the linear channels. It is relevant to stress that asymmetric GS solitons were not reported in previously studied versions of nonlinear systems with KP potentials [11, 12, 22], although some exact asymmetric solutions for non-fundamental solitons, which feature nodes, were found in Ref. [11].

With the further increase of the power, the GS soliton undergoes strong self-compression, which eliminates all side peaks, while the central peak moves from the linear stripe into an adjacent nonlinear one, ending up in the middle of the nonlinear stripe. As seen in Fig. 2(c), in the corresponding moderately nonlinear regime the single-peak soliton eventually restores its symmetry about the midpoint of the nonlinear channel into which it has shifted. Accordingly, light is guided by the nonlinear stripe in this regime.

Finally, in the strongly nonlinear regime the *second* SSB event happens, as seen in Fig. 2(d), where the narrow GS soliton spontaneously shifts from the midpoint of the nonlinear stripe, although staying in it. To the best of our knowledge, such a *repeated* SSB of solitons has not been reported in other models of nonlinear optics or BEC. The

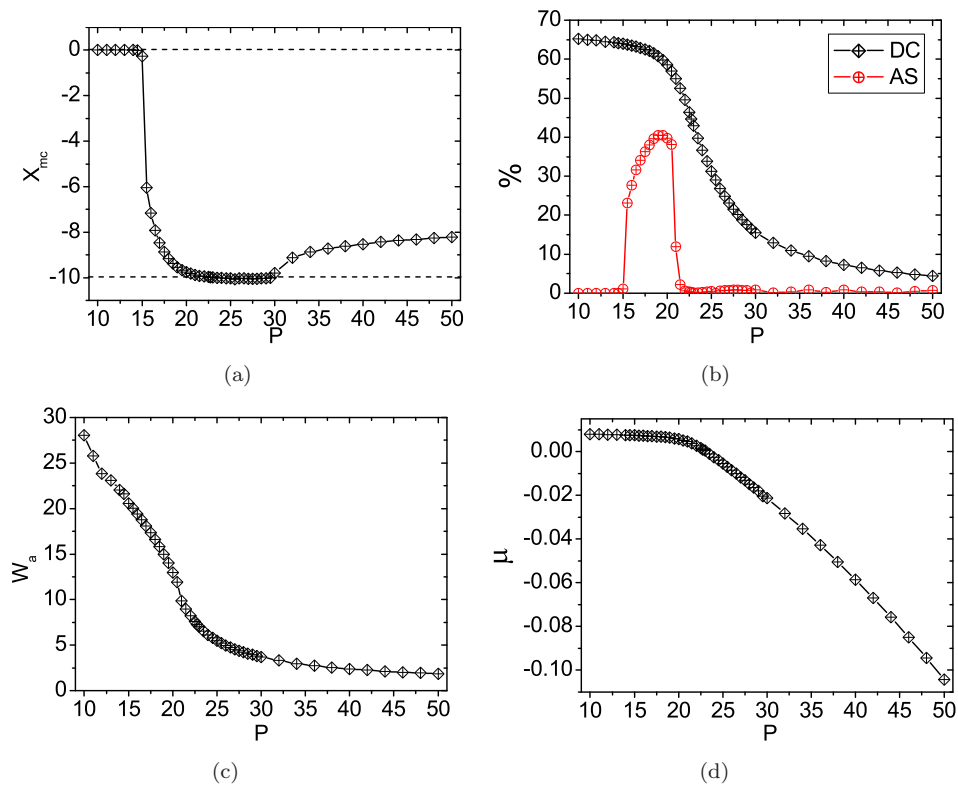


FIG. 3: (Color online) (a) The coordinate of the soliton’s center of mass versus total power P . (b) The duty cycle (DC), showing the share of the power trapped in linear stripes, and the soliton’s asymmetry measure (AS), versus P . (c,d): The soliton’s width (W_a) and propagation constant ($-\mu$) as functions of P (it can be checked that all values of μ belong to the semi-infinite gap, in terms of the spectrum of the linearized system). Note that the $\mu(P)$ dependence satisfies the Vakhitov-Kolokolov stability criterion [23], $d\mu/dP < 0$.

second SSB seems a counter-intuitive effect, as one might “naively” expect that, with indefinite increase of total power P , the narrow high-power soliton would be only stronger nested at the center of the nonlinear stripe. Nevertheless, an explanation to this effect is possible, as argued below.

To quantify the double SSB, we define the following characteristics of the soliton, as functions of the total power, P : center-of-mass coordinate x_{mc} , average width W_a , linear-stripe duty cycle (DC), the soliton’s asymmetry measure (AS), and the above-mentioned propagation constant, $-\mu$ (if the system is realized as the BEC model, μ is the chemical potential):

$$\begin{aligned}
 x_{mc} &= P^{-1} \int_{-\infty}^{+\infty} x |u|^2 dx, \\
 DC &= P^{-1} \int_{L_s} |u|^2 dx, \quad AS = P^{-1} \int_0^{\infty} \left| [u(x_{max} - y)]^2 - [u(x_{max} + y)]^2 \right| dy, \\
 W_a^2 &= P^{-1} \int_{-\infty}^{+\infty} (x - x_{mc})^2 |u|^2 dx, \quad \mu = P^{-1} \int_{-\infty}^{+\infty} u^* \hat{\mathbf{H}} u dx,
 \end{aligned} \tag{2}$$

where \int_{L_s} stands for the integral taken over the linear stripes, x_{max} is the location of the maximum value of $|u(x)|$, and the Hamiltonian operator is $\hat{\mathbf{H}} = (1/2)\partial_{xx} + V(x)[1 - |u|^2]$. For $DC > 50\%$ ($< 50\%$), light is mainly guided by the linear (nonlinear) stripes. The strength of the SSB as a whole is quantified by shift x_{mc} , while AS quantifies the related inner symmetry breaking of the soliton.

The overall description of the double SSB is provided, in Fig. 3, by plots showing the evolution of quantities (2) with the increase of P . In panel (a), the dashed lines, $x = 0$ and $x = -10$, mark the positions of the two symmetric points in the KP potential, which correspond, respectively, to midpoints of the linear and nonlinear stripes. The plots in Figs. 3(a,b) clearly demonstrate that the low-power GS soliton remains symmetric, being centered at $x = 0$, for $P < 15$.

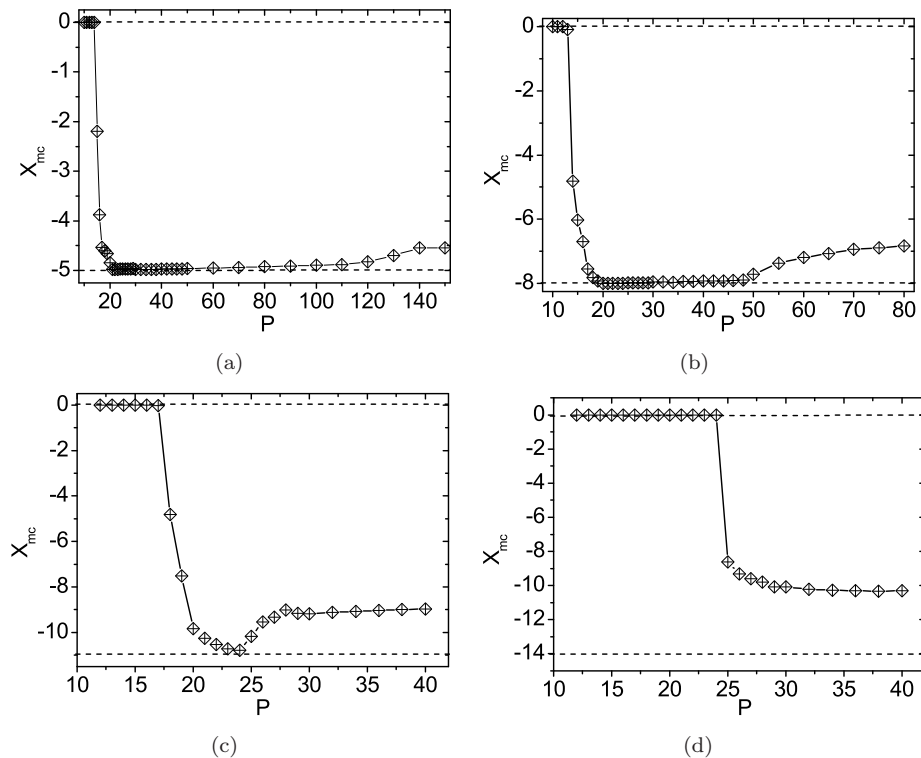


FIG. 4: (Color online) $x_{mc}(P)$ for different value of the lattice period: (a) $d = 5$, (b) $d = 8$, (c) $d = 11$, and (d) $d = 14$

The first SSB event occurs at $P_{SSB}^{(1)} \approx 15$. The soliton becomes asymmetric, gradually moving from the midpoint of the linear stripe ($x = 0$) towards the center of the adjacent nonlinear one ($x = -10$), in the interval of $15 < P < 22$. As seen in Fig. 3(b), the soliton attains the largest inner asymmetry degree, $AS > 40\%$, around $P \simeq 18$. Observe that the asymmetric soliton gradually loses its side peaks, simplifying into the single-peak shape, as seen in Figs. 2(a-c). The dependence $AS(P)$ in Fig. 3(b) shows that the SSB occurring at $P = P_{SSB}^{(1)}$ is of the *supercritical type*, i.e., it may be identified with a phase transition of the second kind [24].

Next, the moderately high-power soliton remains completely symmetric, centered at the midpoint of the nonlinear channel, at $22 < P < 30$. Note also that the duty cycle falls to values $DC < 50\%$ at $P > 22$, which implies the switch from the quasi-linear guidance to that dominated by the nonlinear pseudopotential.

The second SSB occurs at $P_{SSB}^{(2)} \approx 30$. At $P > 30$, the high-power soliton gradually shifts from $x = -10$ towards the edge of the nonlinear stripe, while keeping a virtually undisturbed symmetric shape, with $AS = 0$, see Fig. 3(b). This instance of the SSB may also be considered as a phase transition of the second kind.

B. Extension to other values of the potential's period

To present the most general results, in Fig. 4 we report dependence $x_{mc}(P)$ for different values of d (still with $d_1 = d_2 = d$), *viz.*, $d = 5, 8, 11$, and 14 . We notice that, when d increases from 5 in Fig. 4(a) to 11 in Fig. 4(c), the power at which the second SSB takes place decreases from $P_{SSB}^{(2)} \approx 120$ to $\simeq 24$. This is explained by the fact that the second SSB requires the average width of the soliton to be much narrower than the width of the nonlinear stripe, hence, with smaller d , larger P is needed to sustain the second SSB for a tighter localized soliton. This argument also explains the shrinkage of the interval in which the soliton is pinned to the symmetric position at the midpoint of the the nonlinear stripe with the increase of d , as seen in Figs. 4(a),(b) and (c). If d keeps increasing, this interval eventually disappears at $d > 11$, as shown in Fig. 4(d), pertaining to $d = 14$.

Further, in Fig. 5 we plot soliton characteristics DC , AS and W_a for $d = 14$. It exhibits a direct transition from the original symmetric state to the final asymmetric state, without the second SSB.

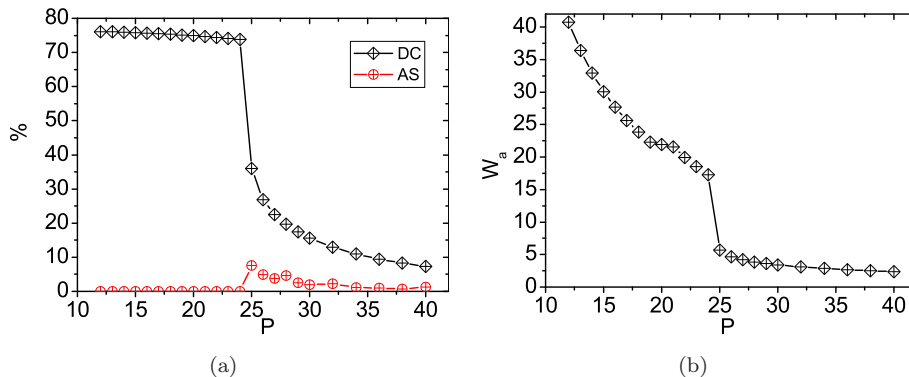


FIG. 5: (Color online) (a) Dependences DC(P) and AS(P) for $d = 14$. (b) $W_a(P)$ for $d = 14$.

III. ANALYTICAL CONSIDERATIONS

Both instances of the SSB revealed by the numerical findings can be explained by means of analytical approximations. To address the first SSB, which happens to the *broad* low-power GS soliton, we replace the KP modulation function with period $D \equiv 2d$ in Eq. (1), $V(x)$ (see Fig. 1), by the combination of its mean value and the first harmonic component, dropping higher-order harmonic components (cf. Ref. [10]):

$$\tilde{V}(x) = (V_0/2) [1 - (4/\pi) \cos(2\pi x/D)], \quad (3)$$

Accordingly, Eq. (1) is replaced by

$$iu_z = -(1/2)u_{xx} + \tilde{V}(x) (1 - |u|^2) u. \quad (4)$$

In the zero-order approximation, one may neglect the variable part of the modulation function, whose period is much smaller than the width of soliton. In this case, Eq. (4) gives rise to the obvious soliton solution,

$$u(x, z) = \sqrt{2/V_0} \eta e^{ikz} \operatorname{sech}(\eta(x - \xi)), \quad k = \frac{1}{2}(\eta^2 - V_0), \quad (5)$$

with coordinate of the soliton's center ξ and inverse width η . The total power of the soliton is $P = 4\eta/V_0$.

The Hamiltonian corresponding to Eq. (4) is

$$H = \frac{1}{2} \int_{-\infty}^{+\infty} [|u_x|^2 + \tilde{V}(x) [2|u|^2 - |u|^4]] dx. \quad (6)$$

As follows from here, the energy of the interaction of the broad soliton, taken as per Eq. (5) (which neglects the distortion of the soliton's shape under the action of the potential) with the variable part of modulation function (3), expressed in terms of the soliton's power, is

$$\begin{aligned} U(\xi) &\equiv - (V_0/\pi) \int_{-\infty}^{+\infty} \cos(2\pi x/D) [2|u(x)|^2 - |u(x)|^4] dx \\ &= \frac{8\pi}{d} \left[\sinh\left(\frac{4\pi^2}{PV_0D}\right) \right]^{-1} \left[-1 + \frac{2}{3V_0} \left(\left(\frac{\pi}{D}\right)^2 + \frac{P^2V_0^2}{16} \right) \right] \cos\left(\frac{2\pi\xi}{D}\right). \end{aligned} \quad (7)$$

For small P (low-power solitons), energy (7) gives rise to a *local minimum* of the corresponding potential, i.e., a *stable* equilibrium position of the soliton at $\xi = 0$, provided that

$$V_0 > 2\pi^2 / (3D^2). \quad (8)$$

Note that the parameter values adopted above to generate Figs. 1-3, $D = 20$ and $V_0 = 0.02$, satisfy this condition. Then, with the increase of P , the equilibrium position predicted by potential (7) becomes unstable at

$$P > P_{\text{SSB}}^{(1)} \equiv (4/V_0) \sqrt{(3/2)V_0 - (\pi/D)^2}. \quad (9)$$

At $P > P_{\text{SSB}}^{(1)}$, the soliton moves away from $\xi = 0$, i.e., this is the point of the first SSB. Note that, for $V_0 = 0.02$ and $D = 20$, expression (9) yields $P_{\text{SSB}}^{(1)} \approx 14.6$, which practically exactly coincides with the first SSB point identified above from the numerical data, $P_{\text{SSB}}^{(1)} \approx 15$. If D is too small and does not satisfy condition (8) for given V_0 , this means that the simplest approximation cannot be used, and corrections to the average form of the soliton (5) should be taken into account, which is beyond the scope of the present analysis.

Proceeding to the analytical consideration of the second SSB, we rewrite Eq. (1) as

$$iu_z = -(1/2)u_{yy} - V(y) (|u|^2 - 1) u, \quad (10)$$

where coordinate y is defined so as to place the center of the nonlinear stripe at $y = 0$. Aiming to consider narrow solitons, trapped in the given channel, which do not feel the presence of other nonlinear stripes, we define the modulation function here so that $V(y) = V_0$ in the nonlinear stripe, and $V(y) = 0$ outside of it. Then, the narrow soliton with the center located at point $y = \xi$ (generally, shifted off the center of the nonlinear stripe) has the following form:

$$u(z, x) = \frac{\eta e^{ikz}}{\sqrt{V_0}} \begin{cases} \text{sech}(\eta(y - \xi)), & \text{at } |y| < \frac{d_2}{2}, \\ 2 \exp \left[-\eta \left(\frac{d_2}{2} - \xi \text{sgn}(y) \right) - \sqrt{\eta^2 - 2V_0} \left(|y| - \frac{d_2}{2} \right) \right] & \text{at } |y| > \frac{d_2}{2}, \end{cases} \quad (11)$$

where this time the inverse width of the soliton is assumed to be large, $\eta \gg 1/d_2$, k is the same as in Eq. (5), and the total power of the narrow soliton is $P \approx 2\eta/V_0$.

The substitution of the wave field (11) into the Hamiltonian of Eq. (10) yields the following effective potential of the interaction of the soliton with the nonlinear stripe which holds it:

$$U(\xi) = -2\eta \left[\frac{\eta^2}{V_0} \left(1 - \sqrt{1 - \frac{2V_0}{\eta^2}} \right) + 2 \right] e^{-\eta d_2} \cosh(2\eta\xi) + \frac{4\eta^3}{V_0} e^{-2\eta d_2} \cosh(4\eta\xi), \quad (12)$$

cf. Eq. (7). As might be expected, the last term in this potential tends to keep the soliton at the center ($\xi = 0$), while the other terms push it towards the edge of the nonlinear stripe. The equilibrium position is defined by equation $dU/d\xi = 0$. The substitution of potential (12) into this equation yields two solutions: either $\xi = 0$, which corresponds to the soliton placed exactly at the center, and the off-center equilibrium, determined by the following expression:

$$\cosh(2\eta\xi) = \frac{1}{8} \left[\left(1 - \sqrt{1 - \frac{2V_0}{\eta^2}} \right) + \frac{2V_0}{\eta^2} \right] e^{\eta d_2}. \quad (13)$$

Solution (13) exists if it yields $\cosh(2\eta\xi) > 1$, i.e.,

$$e^{\eta d_2} > 8 \left[\left(1 - \sqrt{1 - 2V_0/\eta^2} \right) + 2V_0/\eta^2 \right]^{-1}. \quad (14)$$

Following the assumption that the soliton is narrow, we assume $2V_0/\eta^2 \ll 1$, hence Eqs. (13) and (14) are simplified as follows:

$$\cosh(V_0 P \xi) = 3 (2V_0 P^2)^{-1} \exp(V_0 d_2 P/2), \quad (15)$$

$$\exp(V_0 d_2 P/2) > (2/3) V_0 P^2. \quad (16)$$

The second SSB is realized, in the framework of the present approximation, as the displacement of the soliton from $\xi = 0$ to point (13), hence inequality (16), if replaced by the respective equality, offers a rough approximation for the second SSB point, $P_{\text{SSB}}^{(2)}$ [“rough” because it was derived taking into regard exponentially small terms in Eq. (12), which is a crude but meaningful approximation [25]]. In particular, Eq. (16) predicts that, for $V_0 = 0.02$, the numerically found value reported above, $P_{\text{SSB}}^{(2)} = 30$, corresponds to $d_2 \simeq 8.3$, which is not far from $d_2 = 10$ which was actually used. For $P \rightarrow \infty$, Eq. (15) yields $\xi \rightarrow \pm d_2/2$, i.e., within the framework of the present approximation, the soliton moves to the edge of the nonlinear stripe. On the other hand, for larger values of d_2 inequality (16) always holds, which explains the disappearance of the second SSB in the numerical picture displayed in Fig. 4.

IV. CONCLUSION

We have demonstrated the effect of the double SSB (spontaneous symmetry breaking) for GS (ground-state) stable solitons in the 1D medium with the competing periodic linear potential and its nonlinear counterpart (pseudopotential)

induced by a periodic modulation of the local self-attraction coefficient. This medium may be realized as a virtual PhC (photonic crystal) imprinted by means of the EIT technique into a uniform optical medium, and also as the BEC setting using a combination of an optical lattice and the spatially periodic modulation of the nonlinearity via the Feshbach resonance. The two SSB events occur in the low- and high-power regimes, pushing the soliton off the symmetric positions at the center of the linear and nonlinear stripes, respectively. In the former case, the SSB also affects the shape of the low-power soliton, making it asymmetric and gradually stripping it of side peaks. In the latter case, the narrow high-power soliton, while shifting off the midpoint of the nonlinear channel, keeps the symmetric shape. At intermediate values of the power, the soliton is completely symmetric, staying pinned at the center of the nonlinear stripe. On the other hand, the increase of the period of the potential structure leads to the direct transition from the original symmetric state to the final asymmetric one, while the second SSB point disappears. These results, which were obtained by means of systematic numerical computations and explained with the help of analytical approximations, suggest a possibility to control the switching of spatial optical solitons in the virtual PhC by varying their power.

This work may be extended in other directions. In particular, a challenging problem is to investigate similar settings and effects for 2D solitons, in terms of PhCs and BEC alike.

Y.L. thanks Prof. X. Sun (Fudan University, Shanghai) for a useful discussion. B.A.M. appreciates the hospitality of the State Key Laboratory of Optoelectronic Materials and Technologies at the Sun Yat-sen University (Guangzhou, China), and of the Department of Mechanical Engineering at the Hong Kong University. This work was supported by the Chinese agencies NKBRFS (grant No. G2010CB923204) and CNNSF (grant No. 10934011).

-
- [1] L. D. Landau and E. M. Lifshitz, *Quantum Mechanics* (Moscow: Nauka Publishers, 1974).
- [2] E. B. Davies, *Comm. Math. Phys.* **64**, 191 (1979); J. C. Eilbeck, P. S. Lomdahl, and A. C. Scott, *Physica D* **16**, 318 (1985).
- [3] A. W. Snyder, D. J. Mitchell, L. Poladian, D. R. Rowland, and Y. Chen, *J. Opt. Soc. Am. B* **8**, 2101 (1991).
- [4] C. Paré and M. Florjańczyk, *Phys. Rev. A* **41**, 6287 (1990); A. I. Maimistov, *Kvant. Elektron.* **18**, 758 [*Sov. J. Quantum Electron.* **21**, 687 (1991)]; N. Akhmediev and A. Ankiewicz, *Phys. Rev. Lett.* **70**, 2395 (1993); P. L. Chu, B. A. Malomed, and G. D. Peng, *J. Opt. Soc. A B* **10**, 1379 (1993); B. A. Malomed, in: *Progr. Optics* **43**, 71 (E. Wolf, editor: North Holland, Amsterdam, 2002).
- [5] L. C. Qian, M. L. Wall, S. Zhang, Z. Zhou, and H. Pu, *Phys. Rev. A* **77**, 013611 (2008); T. Maytevarunyoo, B. A. Malomed, and G. Dong, *ibid. A* **78**, 053601 (2008).
- [6] W. A. Harrison, *Pseudopotentials in the Theory of Metals* (Benjamin: New York, 1966).
- [7] L. Pitaevskii and S. Stringari, *Bose-Einstein Condensation* (Clarendon Press: Oxford, 2003).
- [8] P. Xie, Z.-Q. Zhang, and X. Zhang, *Phys. Rev. E* **67**, 026607 (2003); A. Ferrando, M. Zacarés, P. Fernández de Córdoba, D. Binosi, and J. A. Monsoriu, *Opt. Exp.* **11**, 452 (2003); **12**, 817 (2004); J. R. Salgueiro, Y. I. S. Kivshar, D. E. Pelinovsky, V. Simón, and H. Michinel, *Stud. Appl. Math.* **115**, 157 (2005); A. S. Desyatnikov, N. Sagemerten, R. Fischer, B. Terhalle, D. Träger, D. N. Neshev, A. Dreischuh, C. Denz, W. Królikowski, and Y. S. Kivshar, *ibid.* **14**, 2851 (2006).
- [9] Q. Li, C. T. Chan, K. M. Ho and C. M. Soukoulis, *Phys. Rev. B* **53**, 15577 (1996); E. Lidorikis, Q. Li, and C. M. Soukoulis, *ibid.* **54**, 10249 (1996).
- [10] B. A. Malomed, Z. H. Wang, P. L. Chu, and G. D. Peng, *J. Opt. Soc. Am. B* **16**, 1197 (1999).
- [11] Y. Kominis, *Phys. Rev. E* **73**, 066619 (2006); Y. Kominis and K. Hizanidis, *Opt. Exp.* **16**, 12124 (2008).
- [12] Y. Kominis and K. Hizanidis, *Opt. Lett.* **31**, 2888 (2006); T. Maytevarunyoo and B. A. Malomed, *J. Opt. Soc. Am. B* **25**, 1854 (2008).
- [13] A. Gubeskys and B. A. Malomed, *Phys. Rev. A* **75**, 063602 (2007); **A** **76**, 043623 (2007).
- [14] M. Matuszewski, B. A. Malomed, and M. Trippenbach, *Phys. Rev. A* **75**, 063621 (2007); M. Trippenbach, E. Infeld, J. Gocalek, M. Matuszewski, M. Oberthaler, and B. A. Malomed, *ibid. A* **78**, 013603 (2008).
- [15] N. V. Hung, P. Ziñ, M. Trippenbach, and B. A. Malomed, *Phys. Rev. E* **82**, 046602 (2010).
- [16] C. Hang and V. V. Konotop, *Phys. Rev. A* **81**, 053849 (2010); Y. Li, B. A. Malomed, M. Feng, and J. Zhou, *ibid.* **82**, 633813 (2010).
- [17] H. Sakaguchi and B. A. Malomed, *Phys. Rev. A* **81**, 013624 (2010).
- [18] Y. V. Kartashov, V. A. Vysloukh, and L. Torner, in: *Progr. Optics* **52**, 63 (E. Wolf, editor: North Holland, Amsterdam, 2009).
- [19] Y. V. Kartashov, B. A. Malomed, and L. Torner, *Solitons in nonlinear lattices*, *Rev. Mod. Phys.*, in press.
- [20] F. Lederer, G. I. Stegeman, D. N. Christodoulides, G. Assanto, M. Segev, and Y. Silberberg, *Phys. Rep.* **463**, 1 (2008).
- [21] M. L. Chiofalo, S. Succi, and M. P. Tosi, *Phys. Rev. E* **62**, 7438 (2000).
- [22] I. M. Merhasin, B. V. Gisin, R. Driben, and B. A. Malomed, *Phys. Rev. E* **71**, 016613 (2005).
- [23] M. Vakhitov and A. Kolokolov, *Radiophys. Quantum. Electron.* **16**, 783 (1973); L. Bergé, *Phys. Rep.* **303**, 259 (1998).
- [24] L. D. Landau and E. M. Lifshitz, *Statistical Physics* (Moscow: Nauka Publishers, 1976).
- [25] Yu. S. Kivshar and B. A. Malomed, *Phys. Rev. Lett.* **60**, 164 (1988); *Rev. Mod. Phys.* **61**, 763 (1989).